



OPEN

All-electrical deterministic single domain wall generation for on-chip applications

SUBJECT AREAS:

MAGNETIC DEVICES

SPINTRONICS

MAGNETIC PROPERTIES AND
MATERIALS

Chinkhanlun Guite, I. S. Kerk, M. Chandra Sekhar, M. Ramu, S. Goolaup & W. S. Lew

School of Physical and Mathematical Sciences, Nanyang Technological University, 21 Nanyang Link, Singapore 637371.

Received
29 September 2014Accepted
24 November 2014Published
12 December 2014Correspondence and
requests for materials
should be addressed to
W.S.L. (wensiang@
ntu.edu.sg)

Controlling domain wall (DW) generation and dynamics behaviour in ferromagnetic nanowire is critical to the engineering of domain wall-based non-volatile logic and magnetic memory devices. Previous research showed that DW generation suffered from a random or stochastic nature and that makes the realization of DW based device a challenging task. Conventionally, stabilizing a Néel DW requires a long pulsed current and the assistance of an external magnetic field. Here, we demonstrate a method to deterministically produce single DW without having to compromise the pulse duration. No external field is required to stabilize the DW. This is achieved by controlling the stray field magnetostatic interaction between a current-carrying strip line generated DW and the edge of the nanowire. The natural edge-field assisted domain wall generation process was found to be twice as fast as the conventional methods and requires less current density. Such deterministic DW generation method could potentially bring DW device technology, a step closer to on-chip application.

Control of magnetic domain wall (DW) dynamics in ferromagnetic nanowires has received increasing research interest due to its potential applications in non-volatile logic devices^{1,2}, magnetic memory^{2–6} and sensors⁷. To translate domain wall-based laboratory device into workable memory product, the mechanisms of injection, driving and detection of magnetic DW must necessarily be well established. Intensive investigations have been carried out to overcome the high current density requirement for current-induced DW driving^{8–13}. The detection by ultrasensitive magnetic tunnel junction sensors are considered relatively well established. However, the DW injection mechanism is not yet fully controlled^{8,11,14,15}. In the reported research of the DW injection mechanisms, a direct application of external magnetic field was naturally the simplest approach to create a DW^{16–18}. This method lacks the capability of individual DW manipulation, and is a slow process¹⁴. DW generation via the localized switching of magnetization using the Oersted field generated by a current-carrying strip line which is transverse to the nanowire^{15,19–21} is now a well-established technique. This is a fast and efficient method in which DW can be created in nanosecond range. However, this method generates a head-to-head (HH) and a tail-to-tail (TT) DWs of opposite magnetic charges on either side of the injection strip line²². Due to their opposite magnetic charge, the DWs attract each other leading to either the formation of a coupled DW, or mutually annihilate each other depending on their topological charges^{14,22,23}. The random nature of the topological charges, leading to DW annihilation results in a stochastic DW generation. For the coupled DW, external magnetic field acting globally on the nanowire or long duration current pulse have been employed to push the two generated DWs apart increasing the generation probability in the process^{15,24}. External magnetic field is not suitable for device application and long duration current pulses generate more heat and affect the power efficiency of a device. Also, multiple current pulses were still required for reliable DW generation as the generation probability is not 100%²⁴. We show that it is possible to generate a single DW with 100% probability without the need of an external magnetic field. This was achieved by exploiting the intrinsic edge stray field of the magnetic nanowire. The edge stray field influences the DWs created by the Oersted field, leading to the annihilation of one of the DWs. This method of single DW generation was found to be twice as fast as conventional method and requires lesser current density.

Results

Two DWs Generation in Zero External Magnetic Field. In-situ anisotropic magnetoresistance (AMR) measurements were used for detection of DW generation. Scanning electron microscope (SEM) image of our device along with the schematic for AMR measurement is shown in Fig. 1a. The nanowire is 300 nm wide with 10 nm thick Ni₈₀Fe₂₀ film. The injection strip line is 800 nm wide with 100 nm thick Au film, and is placed ~ 2 μm away from the nanowire edge. When a current density, $J = 2.6 \times 10^{12} \text{ Am}^{-2}$ was injected through the strip

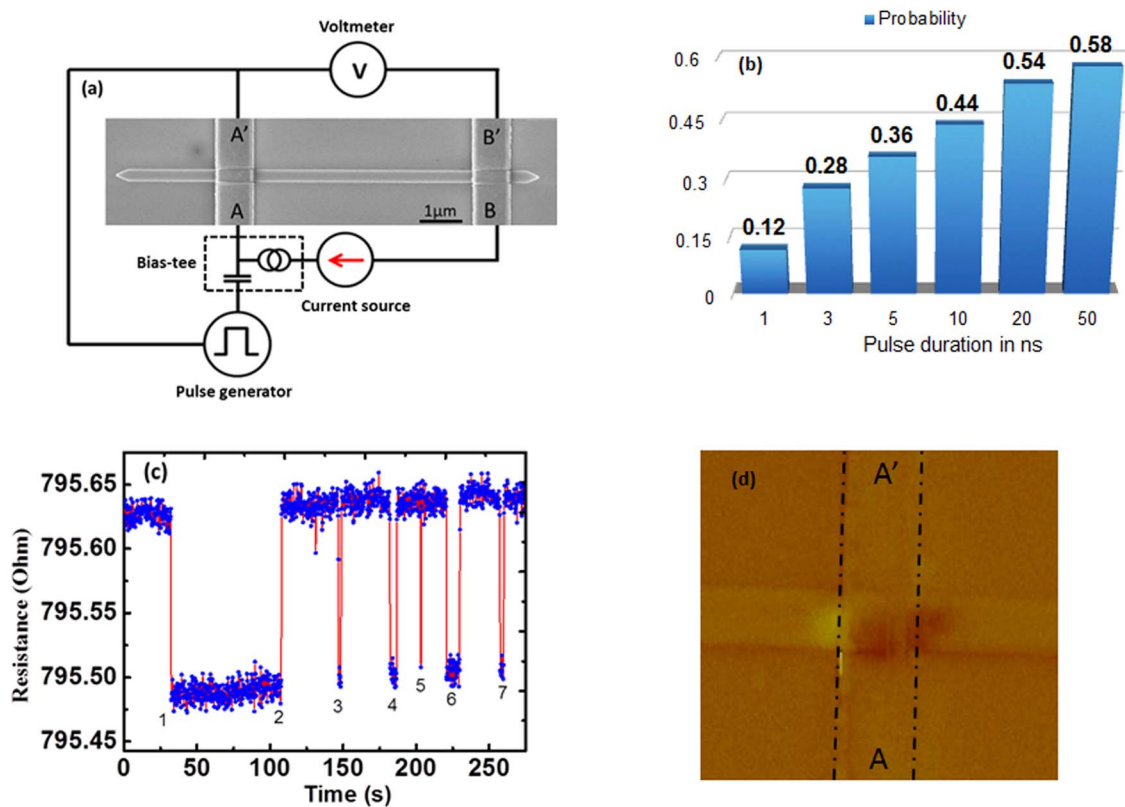


Figure 1 | Conventional DW generation where two DWs are generated by a single injection. (a) Scanning electron microscope (SEM) image of the NiFe DW device with schematic of AMR measurement. (b) Probability of DW generation for applied current density of $2.1 \times 10^{12} \text{ Am}^{-2}$. (c) Measured signals showing successful DW injection followed by several failed injection due to DW-DW annihilation. (d) Shows MFM image of generated DWs beneath the injection strip line.

line from A to A', DW generation was confirmed by a drop in resistance across AA' and BB'. DWs generation was considered to be successful if the drop in resistance is maintained for more than 60 s and can be annihilated by reversed pulsed current. The probability of successful DW generation in 50 attempts for different pulse durations is shown in Fig. 1b. The maximum probability achieved was less than 60% which is for 50 ns pulse duration. Fig. 1c shows sequence of resistance change of the nanowire as a function of time, following multiple attempts of DW injection and annihilation. The initial measured resistance was $795.625 \pm 0.025 \Omega$. Following a current pulse injection at $t = 30 \text{ s}$, the resistance drop to $795.485 \pm 0.025 \Omega$, indicated by marker 1. The resistance drop was $0.14 \pm 0.025 \Omega$ ^{14,19,20}. The resistance drop which was sustained for more than 60 s indicates a successful DW generation. At $t = 110 \text{ s}$, an applied reversed current restored the nanowire resistance back to its initial value, as shown by marker 2. Further attempts with the same current pulse could not repeat the stable resistance change. Markers 3, 4, 5, 6 and 7 show visible drops in resistance but they last only for a certain period, ranging from milliseconds to a few seconds. This is likely due to the mutual annihilation of generated DWs. The successful DW generation was also directly observed using magnetic force microscope (MFM) imaging as seen in Fig. 1d. The MFM image shows two coupled DWs under the strip line. Driving of the DWs was attempted with current density, $J = 1.3 \times 10^{12} \text{ Am}^{-2}$ in zero external magnetic field without any success. The reason could be because a very small fraction of the current interacts with the DWs due to shunting by the strip line.

There are few issues that are observed in this experiment where two DWs are generated and no external magnetic field was applied. Firstly, the probability of DW generation was less than 100%. This

means that to ascertain DWs generation, more than one current pulse is required²⁴. Additionally, when the DWs generation was successful, they remain beneath the strip line. This makes driving of the DW difficult as only a fraction of the driving current will interact with the DW.

Single DW Generation and Driving in Zero External Magnetic Field. SEM image of the device that allows edge field-assisted single DW generation is shown in Fig. 2a. The 800-nm-wide strip line was positioned 450 nm away from the edge of the nanowire. The magnetic nanowire was saturated with 1 kG field along the wire long axis. A current density of $J = 1.1 \times 10^{12} \text{ Am}^{-2}$ with pulse duration 5 ns was injected into the strip line from A to A'. DW generation was confirmed by a drop in the resistance whose magnitude was similar to the two DWs generation method. After observing the DW generation by *in situ* AMR measurement, it was confirmed using magnetic force microscope (MFM) imaging which is shown in Fig. 2b. A DW which is a few nanometres away from the injection strip line AA' is seen in the image. This confirms the single DW generation. The DW closer to the nanowire edge was annihilated. Edge field assisted single DW generation probability was studied for different current densities ranging from $6.9 \times 10^{11} \text{ Am}^{-2}$ to $1.1 \times 10^{12} \text{ Am}^{-2}$. The pulse duration was varied from 1 to 100 ns. The probabilities for each current density and pulse duration are as shown in Fig. 2c. The probabilities were calculated for 50 attempts. The condition for successful single DW generation was the same as the two DWs generation. 100% single DW generation probabilities were observed for current density of $1.0 \times 10^{12} \text{ Am}^{-2}$ and $1.1 \times 10^{12} \text{ Am}^{-2}$ when their pulse duration exceeds 20 ns and 10 ns respectively for this particular device.

The generated single DW in Fig. 2b was driven with a current density, $J = 1.3 \times 10^{12} \text{ Am}^{-2}$ and pulse width of 10 ns, two pulses

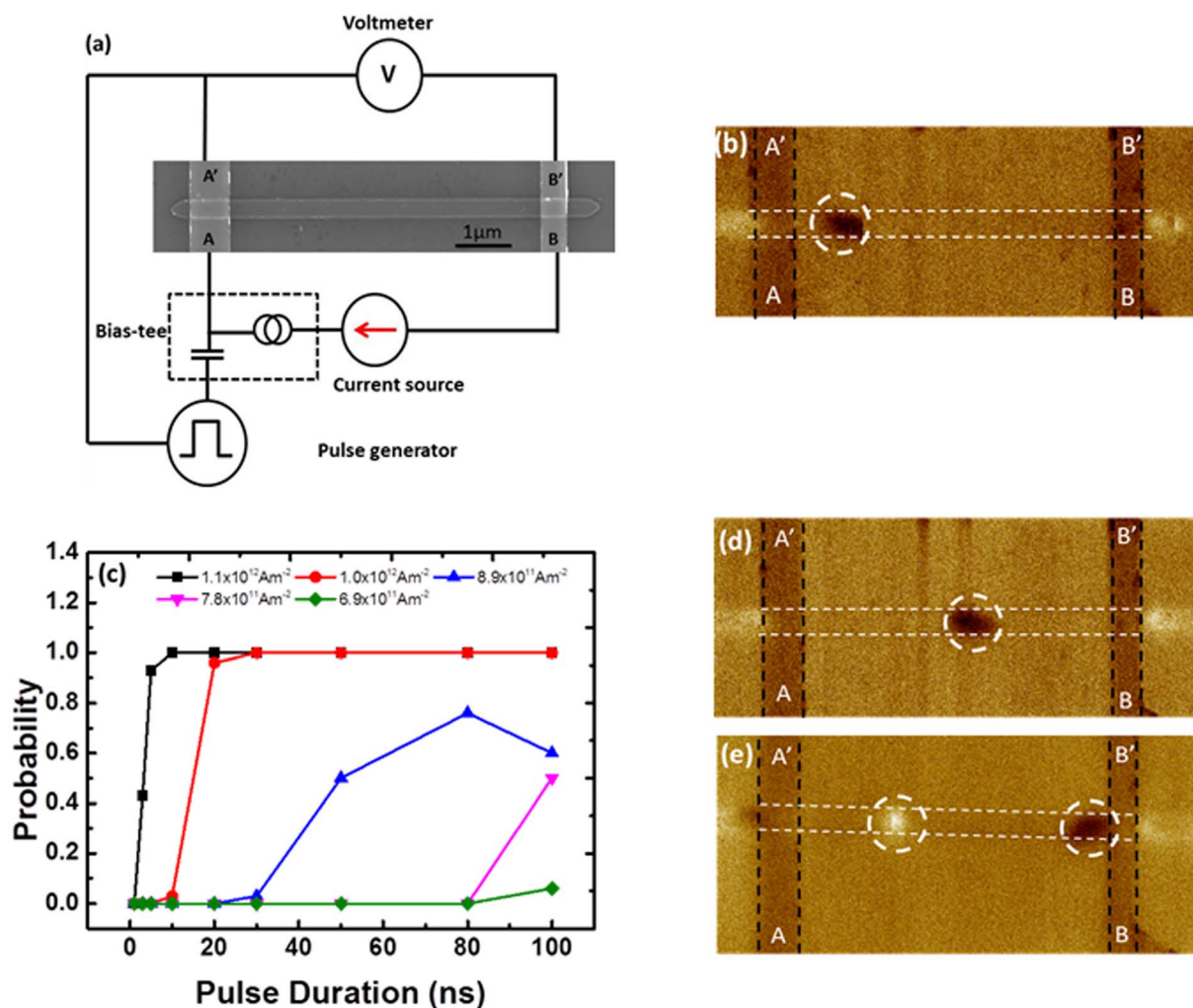


Figure 2 | Single DW generation. (a) SEM image of the modified DW injection device. The injection strip line was positioned at 450 nm away from the nanowire left end point (edge). (b) MFM image of the device showing injected single domain wall. (c) Injection probability of a single domain wall as a function of pulse width for a range of applied current densities. (d) MFM image of the device showing the current-driven DW after a deterministic injection. (e) MFM image of two deterministically-injected DWs in the NiFe nanowire.

were injected. An MFM image of the device confirms that the displacement of the DW from its initial position was $\sim 2 \mu\text{m}$ as shown in Fig. 2d. A second DW was generated by injecting current pulse with current density, $J = 1.1 \times 10^{12} \text{ Am}^{-2}$ and pulse duration 5 ns for A' to A . It was confirmed using MFM imaging as shown in Fig. 2e.

The experimental results showed that it is possible to have 100% DW generation probability. Unlike two DWs generation experiment, mutual annihilation was not observed during *in-situ* AMR measurement. The failed attempt for DW generation simply did not show any resistance change. This confirms that every time there is a success in nucleation, a single DW was generated. This eliminates the mutual annihilation of DWs generated during injection. This allows for 100% generation probability above a certain value of current density and pulse duration. Another advantage is that, the generated single DW is always outside the injection strip line. This makes current driving possible and easy because all the current that passes through the nanowire interacts with the DW.

Study of Single DW Generation Using Micromagnetic Simulation.

To further understand and extrapolate our experimental studies, micromagnetic simulations were performed using Landau-Lifshitz-Gilbert (LLG) simulator (M. R. Scheinfein, LLG Micromagnetics Simulator, <http://llgmicro.home.mindspring.com/>). The spins state evolution of DW nucleation for different distance d between the

edge of the nanowire and the injection strip line is shown in Fig. 3a. The nanowire width was 300 nm with thickness of 10 nm and the strip line width was $1 \mu\text{m}$. A pulsed current density, $J = 1 \times 10^{12} \text{ Am}^{-2}$ with a pulse width of 1 ns was injected into the strip line. The rise and fall time of the current pulse was 300 ps. Initially two DWs were nucleated underneath the strip line in all the configurations. In particular, when the strip line is aligned with the edge of the nanowire, i.e. $d = 0$, only one DW survives by the time the injection pulse was completed. One of the DW was pushed to the edge of the nanowire and was annihilated. The other DW was pushed towards the centre of the nanowire and away from the strip line.

As the distance between the strip line and the edge of the nanowire was increased, i.e., $d = 100 \text{ nm}$ and 200 nm , stabilization of the DW takes longer. Additionally, the single DW generated forms underneath the injection strip line. At $d = 300 \text{ nm}$, the nucleation of domain walls collapsed and no well-defined DWs are nucleated. When the pulse duration was increased to 1.5 ns, single DW generation was successfully achieved for $d = 300 \text{ nm}$. Fig. 3b shows the plot of minimum current density required to generate single DW for different values of d . The current pulse duration was kept constant at 1 ns. The minimum current density required increases linearly up to $d \approx 500 \text{ nm}$. For, $d > 500 \text{ nm}$ the minimum current density required remains constant. Fig. 3c shows the plot of the time needed to generate single DW. It

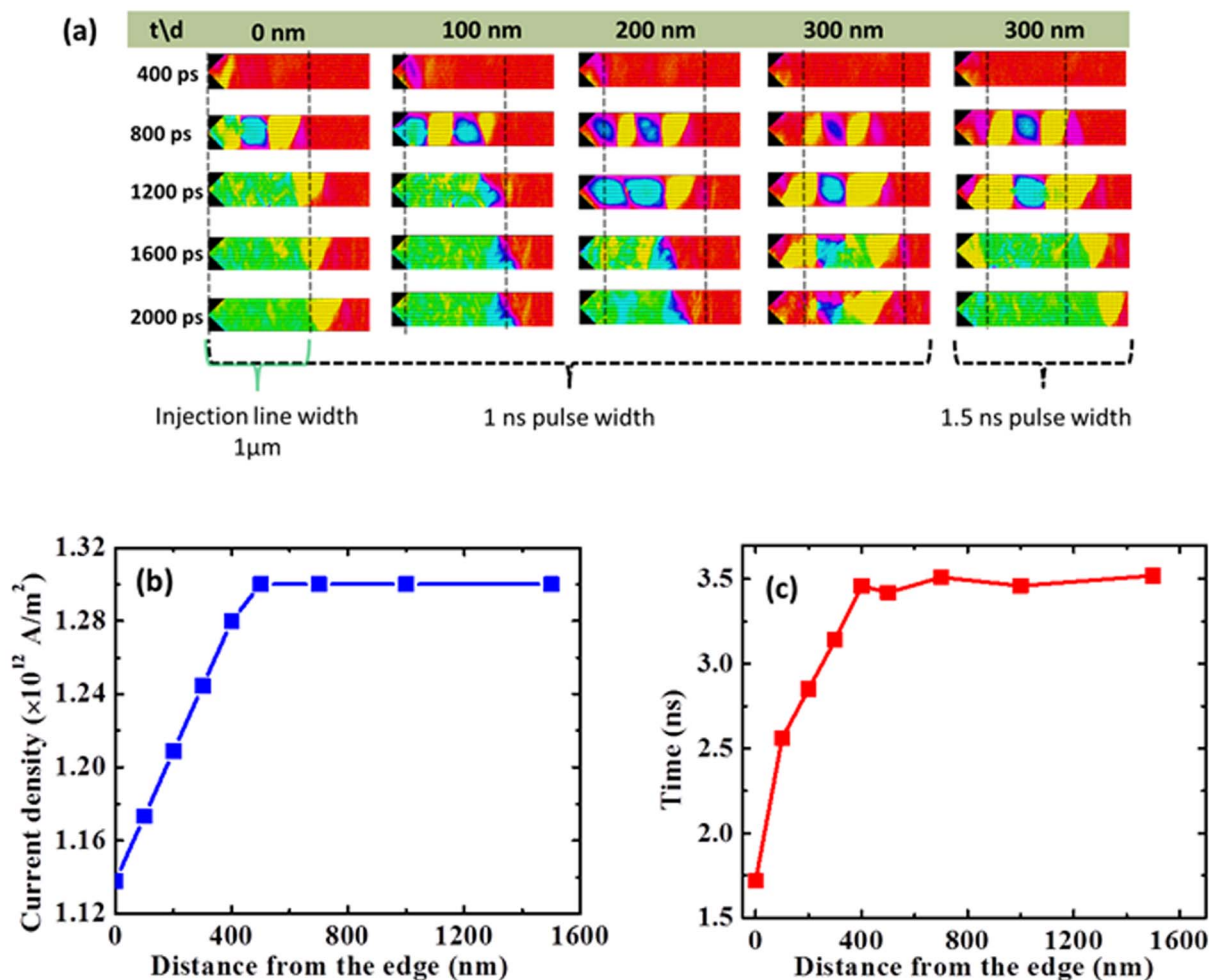


Figure 3 | Simulation for single DW injection. (a) Simulation results show the evolution of DW generation with time, t for different nanowire edge and strip line distance, d . (b) Plot shows the correlation between the current density required for successful DW generation and the distance, d with constant pulse duration. (c) Plot shows the correlation between the domain formation time and the distance, d with constant pulse duration and current density.

increases with increase in d . Similar to Fig. 3b, the required time became constant when $d > 500$ nm.

Simulation Analysis. As the strip line distance d from the nanowire edge was gradually increased from 0 to 200 nm, the DW nucleation time increases and remains underneath the strip line for a longer period of time. This is due to the decrease in the edge field's influence on the generated DWs allowing the mutual interaction between the two to be more pronounced. A more complex reversal process underneath the strip line was observed as the edge stray field influence weakens. At $d = 300$ nm in Fig. 3a, DW was successfully generated when the pulse duration was increased from 1 ns to 1.5 ns without increasing the current density. The Oersted field from the strip line was sustained for a longer period of time, enabling the DW to be pushed closer to the edge. This allows the influence of the edge field on the DW closer to it to become stronger leading to its fast annihilation at the edge. This results in single DW generation.

The weakening of the edge field strength as d increases can be compensated by increasing the current density as shown in Fig. 3b. From Fig. 3c, we note that as the edge stray field decreases due to distance from the injection strip line, the DW evolution time increases. The saturation in Fig. 3b and 3c indicates that the edge stray field effect on the DW generation is effective only for distance, $d < 500$ nm. The nucleation time for $d = 0$ nm, *i.e.* 1.75 ns, as compared to that of $d > 500$ nm, *i.e.* 3.5 ns, implies that the edge field-assisted single DW generation is twice as fast as without the edge field

assistance. The critical current density required when $d = 0$, *i.e.* $1.14 \times 10^{12} \text{ Am}^{-2}$ is also smaller than the critical current density required when $d > 500$ nm, *i.e.* $1.3 \times 10^{12} \text{ Am}^{-2}$. The simulation provides a qualitative analysis of the DW nucleation, as ideal conditions are used in simulation.

Discussion

In these experiments, the stochastic nature of DW generation was contributed by two phenomena namely; DW nucleation and mutual annihilation of the nucleated DWs¹⁴. The contribution by the former was overcome when the local Oersted field generated by the injection current exceeds a certain value called the threshold value. These values were observed for current density, $J = 1.0 \times 10^{12} \text{ Am}^{-2}$ and $1.1 \times 10^{12} \text{ Am}^{-2}$ when their pulse duration are ~ 20 ns and ~ 10 ns respectively for our particular device. The later can be overcome if the pair of DWs generated by the strip line can be pushed $\sim 2.5 \mu\text{m}$ apart^{5,22} or one of the DWs is annihilated during nucleation eliminating the chance of mutual interaction. We have attempted the later and demonstrated an approach to generate a single DW with 100% probability by controlling the stray field magnetostatic interaction between DWs and the edge of nanowire. The existing technique²⁴ requires 100 pulses to ensure reliable DW generation. The edge field assisted single DW generation requires only a single pulse for DW injection because its probability is 100%. Also, the issue of electric current shunting by the injection strip line was overcome without the requirement of long current pulse or an external global



magnetic field. Therefore, edge field assisted single DW generation technique has shown the improvements of reliability, robustness and lesser current density requirement, bringing the on-chip application of DW devices a step closer to actual realization.

Methods

Device fabrication. A silicon wafer with a 300-nm-thick thermally-grown SiO₂ layer was used as a substrate for device fabrication. It was cleaned using Acetone followed by iso-propanol in ultrasonication. A thin film stack of Ta(3 nm)/Ni₈₀Fe₂₀(10 nm)/Ta(3 nm) was deposited using ultrahigh vacuum magnetron sputtering deposition technique. The bottom and top Ta layers were used for seeding and capping respectively. Negative resist ma-N 2403 (Micro Resist Technology) was used for spin coating followed by electron beam lithography patterning. A Ta/NiFe/Ta nanowire pattern with sharp side wall was obtained after argon ion milling and resist stripping processes. To fabricate electrical strip lines and contact pads, the nanowire sample underwent another process of nanolithography. Positive resist para-Methoxymethamphetamine (PMMA) was used for spin coating followed by electron beam lithography patterning. A bilayer Ta(5 nm)/Au(120 nm) stack was deposited onto the resist windows using high vacuum magnetron sputtering technique. Argon reverse sputtering was briefly employed before the contact layer sputtering deposition so as to obtain a better interface. A complete device was obtained after a metal lift-off process with the aid of warm acetone and ultrasonic agitation.

Electrical Measurements. Domain wall injection and resistance measurements were carried out on a 40 GHz-capable probe station (Cascade Microtech). A programmable pulse generator (Picosecond 10300B) is connected to a radio frequency (RF) probe for injecting and driving the domain wall, as schematically shown in Fig. 1a and Fig. 2a. A voltmeter (Keithley 2000) and a constant current source (Keithley 2400) were used to measure the anisotropic magnetoresistance (AMR) of the nanowire. A bias tee was used to isolate the pulse generator from the dc source. For DW generation, the sample was initially saturated with a 1 kG magnetic field along the wire long axis. The potential difference across the nanowire (AA' to BB') was directly measured *via* dc probes while biasing with 100 μ A current. The biasing current was comparatively small as compared to the driving current and does not affect the experiment. For DW generation a current density of the order of 10^{12} Am⁻² was injected from A to A'. The voltage reading of the voltmeter drops when the DW is successfully generated. The voltage reading was observed for over a minute to ascertain stable domain wall injection. If the domain wall survives for this duration, it was considered a successful DW generation. By changing the current density polarities, *i.e.* injecting from A' to A, the generated domain wall can be annihilated. This process was repeated for 50 times each for recording the probability of the DW generation.

For domain wall driving, a current was passed from BB' to AA' of the device shown in Fig 2a such that the electrons flows from AA' to BB'. A constant bias current of 500 μ A was passed through the nanowire from BB' to AA', using a current source. The driving current density was 1.3×10^{12} Am⁻² with a pulse duration of 10 ns.

Micromagnetic Simulations. LLG micromagnetics simulator was used to perform the simulation to support and extrapolate our experimental results. The material parameters were chosen for Ni₈₀Fe₂₀. The anisotropy constant, K was taken as 0, saturation magnetization (M_s) was taken to be 8.6×10^5 Am⁻¹ and the exchange stiffness constant (A) was taken as 1.3×10^{-11} Jm⁻¹. The damping constant (α) value was taken as 0.01 and the non-adiabatic spin-torque constant (β) value was taken as 0.04²⁵. The dimensions of the nanowire are: length 10 μ m, width 300 nm and thickness 10 nm. The injection strip line was modelled as having 1 μ m width with a conducting non-magnetic film thickness of 30 nm. For the DW injection in fig. 3a, a current density of 1×10^{12} Am⁻² with a pulse duration of 1 ns was applied. The rise and fall time was considered to be 300 ps. The pulse duration was increased to 1.5 ns for $d = 300$ nm, when DW fails to generate. For the simulation results presented in fig. 3b the pulse duration was fixed at 2 ns while changing the current density and the distance d . In Fig. 3c, the DW generation time was taken as the time taken for the DW to move out of the injection pad. For this simulations, the pulse duration was taken as 3 ns and the current density was 1×10^{12} Am⁻².

1. Stamps, R. L. *et al.* The 2014 Magnetism Roadmap. *J. Phys. D: Appl. Phys.* **47**, 333001 (2014).
2. Allwood, D. A. *et al.* Magnetic domain-wall logic. *Science* **309**, 1688–1692 (2005).
3. Parkin, S. S. P., Hayashi, M. & Thomas, L. Magnetic domain-wall racetrack memory. *Science* **320**, 190–194 (2008).
4. Franken, J. H., Swagten, H. J. M. & Koopmans, B. Shift registers based on magnetic domain wall ratchets with perpendicular anisotropy. *Nat. Nanotech.* **7**, 499–503 (2012).
5. Hayashi, M., Thomas, L., Moriya, R., Rettner, C. & Parkin, S. S. P. Current-controlled magnetic domain-wall nanowire shift register. *Science* **320**, 209–211 (2008).
6. Jiang, X. *et al.* Enhanced stochasticity of domain wall motion in magnetic racetracks due to dynamic pinning. *Nat. Comm.* **1**, 25 (2010).

7. Weiss, R., Mattheis, R. & Reiss, G. Advanced giant magnetoresistance technology for measurement applications. *Meas. Sci. Technol.* **24**, 082001 (2013).
8. Yamaguchi, A. *et al.* Real-space observation of current-driven domain wall motion in submicron magnetic wires (vol 92, pg 077205, 2004). *Phys. Rev. Lett.* **96**, 179904 (2006).
9. Hayashi, M. *et al.* Current driven domain wall velocities exceeding the spin angular momentum transfer rate in permalloy nanowires. *Phys. Rev. Lett.* **98**, 037204 (2007).
10. Meier, G. *et al.* Direct imaging of stochastic domain-wall motion driven by nanosecond current pulses. *Phys. Rev. Lett.* **98**, 187202 (2007).
11. Hayashi, M. *et al.* Dependence of current and field driven depinning of domain walls on their structure and chirality in permalloy nanowires. *Phys. Rev. Lett.* **97**, 207205 (2006).
12. Lewis, E. R. *et al.* Fast domain wall motion in magnetic comb structures. *Nat. Mater.* **9**, 980–983 (2010).
13. Beach, G. SPINTRONICS Beyond the speed limit. *Nat. Mater.* **9**, 959–960 (2010).
14. Bocklage, L., Stein, F. U., Martens, M., Matsuyama, T. & Meier, G. Time structure of fast domain wall creation by localized fields in a magnetic nanowire. *Appl. Phys. Lett.* **103**, 092406 (2013).
15. Prieto, J. L., Munoz, M. & Martinez, E. Structural characterization of magnetic nanostripes by fast domain wall injection. *Phys. Rev. B* **83**, 104425 (2011).
16. Kunz, A. & Reiff, S. C. Dependence of domain wall structure for low field injection into magnetic nanowires. *Appl. Phys. Lett.* **94**, 192504 (2009).
17. Ahn, S. M. & Moon, K. W. Enhanced controllability of domain-wall pinning by asymmetric control of domain-wall injection. *Nanotechnology* **24**, 105304 (2013).
18. Vernier, N., Allwood, D. A., Atkinson, D., Cooke, M. D. & Cowbu, R. P. Domain wall propagation in magnetic nanowires by spin-polarized current injection. *Europhys. Lett.* **65**, 526–532 (2004).
19. Hayashi, M., Thomas, L., Rettner, C., Moriya, R. & Parkin, S. S. P. Direct observation of the coherent precession of magnetic domain walls propagating along permalloy nanowires. *Nat. Phys.* **3**, 21–25 (2007).
20. Munoz, M. & Prieto, J. L. Suppression of the intrinsic stochastic pinning of domain walls in magnetic nanostripes. *Nat. Comm.* **2**, 562 (2011).
21. Pushp, A. *et al.* Domain wall trajectory determined by its fractional topological edge defects. *Nat. Phys.* **9**, 505–511 (2013).
22. Thomas, L., Hayashi, M., Moriya, R., Rettner, C. & Parkin, S. Topological repulsion between domain walls in magnetic nanowires leading to the formation of bound states. *Nat. Comm.* **3**, 810 (2012).
23. Stein, F. U., Bocklage, L., Matsuyama, T. & Meier, G. Generation and annihilation of domain walls in nanowires by localized fields. *Appl. Phys. Lett.* **100**, 192403 (2012).
24. Annunziata, A. J. *et al.* Racetrack Memory Cell Array with Integrated Magnetic Tunnel Junction Readout. *2011 IEEE International Electron Devices Meeting (IEDM)*, Washington DC. IEEE. DOI:10.1109/IEDM.2011.6131604 (2011, Dec. 5–7).
25. Lepadatu, S. *et al.* Domain-wall pinning, nonadiabatic spin-transfer torque, and spin-current polarization in permalloy wires doped with vanadium. *Phys. Rev. B* **81**, 020413 (2010).

Acknowledgments

This work is supported by the Singapore National Research Foundation CRP grant (Non-volatile memory and logic integrated circuit devices, NRF-CRP9-2011-01). Support from MOE-AcRF Tier 2 grant (MOE2013-T2-2-017) is also acknowledge.

Author contributions

C.G. developed the edge stray field assisted single DW injection technique and analysed the measurement results. M.C.S. performed the micromagnetic simulations and analysed the results. I.S.K. and M.R. fabricated the devices and performed the measurements. C.G., M.C.S., S.G. and W.S.L. wrote the manuscript. The study was supervised by W.S.L. All authors contributed to the discussion and preparation of the manuscript.

Additional information

Competing financial interests: The authors declare no competing financial interests.

How to cite this article: Guite, C. *et al.* All-electrical deterministic single domain wall generation for on-chip applications. *Sci. Rep.* **4**, 7459; DOI:10.1038/srep07459 (2014).



This work is licensed under a Creative Commons Attribution-NonCommercial-NoDerivs 4.0 International License. The images or other third party material in this article are included in the article's Creative Commons license, unless indicated otherwise in the credit line; if the material is not included under the Creative Commons license, users will need to obtain permission from the license holder in order to reproduce the material. To view a copy of this license, visit <http://creativecommons.org/licenses/by-nc-nd/4.0/>